Microfluidics Hot Paper

A Platform for Stop-Flow Gradient Generation to Investigate Chemotaxis

Zuyao Xiao[+], Audrey Nsamela[+], Benjamin Garlan, and Juliane Simmchen*

Abstract: The ability of artificial microswimmers to respond to external stimuli and the mechanistical details of their origins belong to the most disputed challenges in interdisciplinary science. Therein, the creation of chemical gradients is technically challenging, because they quickly level out due to diffusion. Inspired by pivotal stopped flow experiments in chemical kinetics, we show that microfluidics gradient generation combined with a pressure feedback loop for precisely controlling the stop of the flows, can enable us to study mechanistical details of chemotaxis of artificial Janus micromotors, based on a catalytic reaction. We find that these copper Janus particles display a chemotactic motion along the concentration gradient in both, positive and negative direction and we demonstrate the mechanical reaction of the particles to unbalanced drag forces, explaining this behaviour.

Introduction

Starting in the 1940s, stopped flow methods enabled the study of fast chemical kinetics and were thereby pivotal for the understanding of the time dependence in reactions by increasing the time resolution.[1,2] Coupled with spectroscopic techniques, this new strategy quickly dominated the study of enzymatic reactions and influenced the general knowledge on kinetics. Furthermore, stopping the external inflow was quickly found to be a versatile utility and was later adapted to completely different areas of science; to access a variety of shapes in microfluidic synthesis, the Doyle group developed a strategy based on stopping a flow of oligomers before using a shadow mask and UV light to polymerize an array of particles into it: stop flow lithography

was born.[3] A few decades after the development of stopped flow techniques, manipulating small volumes of fluids became a research field in itself, coined microfluidics.[4] Developments such as valves, sensors and pressure controllers have, jointly with improved computational facilities and coupling options, expanded the environments that can be created using controlled flows. In particular, the generation of gradients in microfluidics has been of growing interest for the active matter community.[5] Microfluidics was optimized in flowing conditions and stopping the flow was usually slow and frequently led to backflows or circulating media. Depending on the pumping mechanism and the rigidity of the employed materials to create chambers and tubes, this effect can be significant. Therefore, the generation of microfluidic gradients is frequently overlaid by the effects of flowing matter.

Taking a closer look at survival strategies of most living creatures on earth, from bacteria to humans, one of the common traits is migration to search for food. However, at the microscale, and especially in non-equilibrium physical phenomena, many things differ from the macro world; mass and heat transfer are enhanced, viscous forces are dominant over inertial forces, that is by definition a low Reynolds number regime, and thermal fluctuations become non-negligible.

Bacteria are the most studied prokaryotic entities and are often used as model biological microswimmers in the field of active matter. Even though randomness is constantly introduced via Brownian motion and thereby part of the process, bacteria do have the ability to sense and get attracted to certain chemicals: this is called positive chemotaxis. For bacteria, the underlying mechanism is assumed to be strongly based on transduction of sensed signals,[6,7] but there might also be a purely physical contribution.[8] This behavior, jointly with negative chemotaxis, where microorganisms migrate away from a potentially harmful chemical, is found in other types of biological microswimmers and the explanations are as diverse and complex as are these microorganisms.

Also the artificial branch of the field of micro- and nanomotors has demonstrated similar tactic behaviors,[9–12] with chemotaxis being one of the earliest studied principle for self-propelled Janus particles and tubular micromotors.[13] To understand how can this attraction to nutrients be mimicked by man-made microswimmers, even though they are deprived of any complex receptors, and to disentangle and model the separate physical contributions, different chemotaxis assays have been created.[14,15] Along with this question come experimental challenges on how to

[*] Z. Xiao,[+] A. Nsamela,[+] Dr. J. Simmchen
Chair of Physical Chemistry, TU Dresden, 01062 Dresden, Germany
E-mail: juliane.simmchen@tu-dresden.de

A. Nsamela,[+] Dr. B. Garlan
Elvesys SAS, Rue de Charonne 172, 75011 Paris, France

[+] These authors contributed equally to this work.

create a controlled and stable gradient in the vicinity of the microswimmers,[16,17] avoiding other parameters, such as flows or capillarity.

Within this work, we have developed a technically refined strategy for gradient generation in microfluidics combined with a stopped-flow technique to perform a chemotaxis assay with artificial Janus microswimmers. The flow based gradient generation using a pressure controller allows for more control over the linear gradient profile, its slope and position of the interface. Flow control techniques using peristaltic or syringe pumps suffer from a low responsiveness and high pulsatility, which is undesired as flow stability is directly related to gradient stability.[18] Even though pressure pumps combined with flow sensors offer greater responsiveness and flow stability, there is yet no established solution for instantaneously stopping the flow. Here, to precisely stall the flow, a retroactive loop counteracts any backflow by ensuring a net zero pressure difference in the whole system. Removing flows and capillary forces as a variable in our chemotaxis assay ensures a complete observation of the purely physical contributions[19,20] to chemotactic behavior.

Results

Microfluidic Gradient Generation and Stop Flow Performance

The microfluidic setup used to generate the gradient and observe the microswimmers behavior in zero flow conditions is illustrated in Figure 1A. The objective of this setup was to instantaneously stop the flow after a gradient was established under constant flow rate in the main chamber of the microfluidic chip. Two microfluidic valves direct the fluids from the outlet to either the waste or to a retroactive loop. During normal flow conditions, the valves (numbered 2 and 3 in the schematic) passed the fluids to the outlet where no pressure is applied. The stop flow procedure consists of switching the valves′ position to direct the flow into a retroactive loop meeting the inlet lines just ahead of the flow sensors. By applying the same pressure on both inlet reservoirs, the retroactive loops activation ensures a uniform pressure in the whole system, including the microfluidic chamber. The removal of any pressure difference immediately leads to a net zero flow in the system. A description of the automatic sequence is available in Figure S1.

The flow-based concentration gradient is established by enhanced mixing of two fluids joining first in the Y-junction, they are then flowing into a narrow constriction channel that leads to a wider chamber. The mixing time by diffusion (τ_D) is reduced in the constriction channel because of its smaller width (see equation 1).
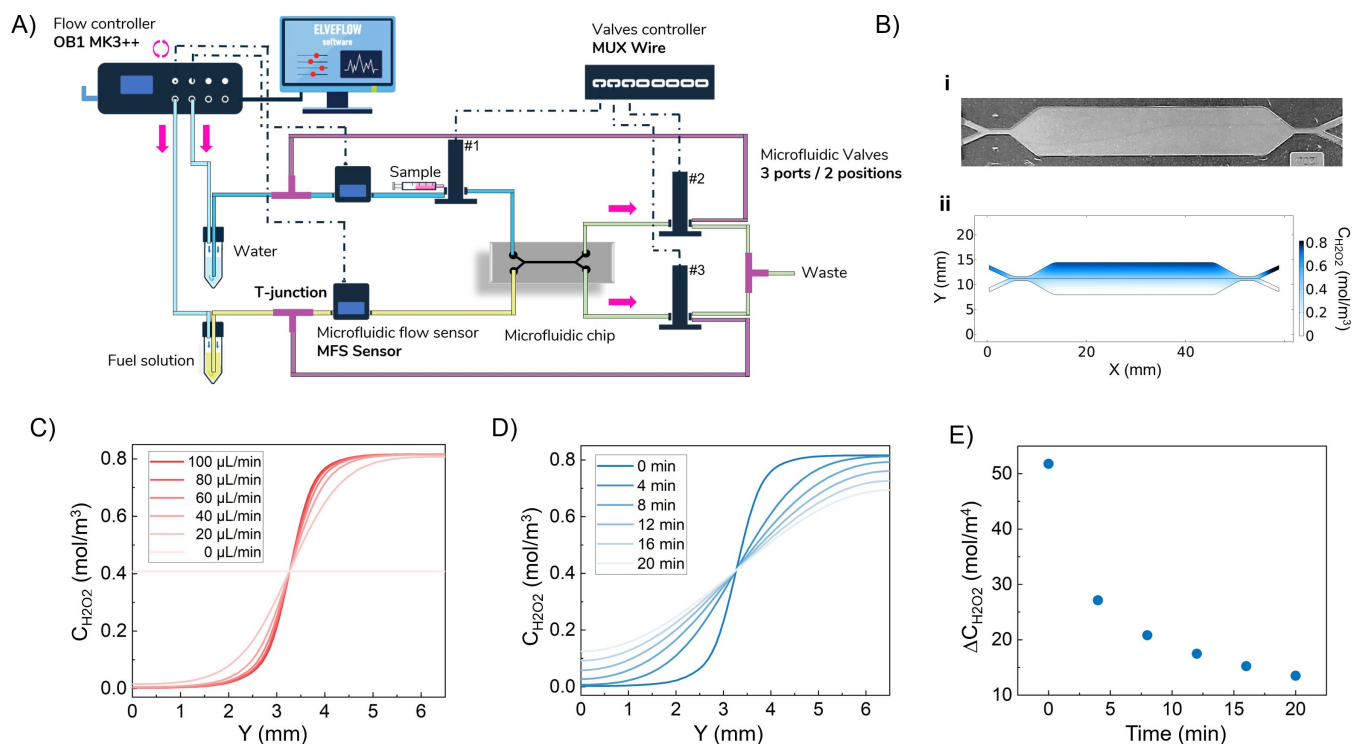

Figure 1. Gradient generation in a microfluidic chip and stop flow performance. (A) Schematic of the experimental setup. (B) Picture of (i) the microfluidic chip and (ii) resulting COMSOL simulations for H_2O_2 concentration profile at $t = 10$ min after stopping the flow, (C) at different flow rates and (D) different time intervals after stop flow actuation. (E) The simulated H_2O_2 concentration gradients as a function of time.

$$\tau_D \approx \frac{L^2}{2D} \qquad (1)$$

where L is the characteristic length (here, the channel width) and D the diffusion coefficient of the reagent. The linear gradient generation in the chip and its evolution after stopping flow actuation was calibrated experimentally using a solution of fluorescein in combination with fluorescence imaging over 10 min after stopping the flow (see Figure S2). Adjusting the flow rates allowed to tune the initial slope of the gradient and a constant flow rate of 80 μL/min was set for both inlet fluids in all experiments. Since fluorescein and hydrogen peroxide have different diffusion coefficients, COMSOL simulations were made to model gradient generation and evolution across the chamber more accurately over time (Figure 1B to E). In less than 5 minutes, the slope of the linear gradient is cut by half as the peroxide diffuses towards the less concentrated region.

Chemotaxis Assay

The microswimmers used in this assay are 5 μm sized silica based Janus particles half coated with copper, that were introduced recently.[21] When these Janus particles are dispersed in H_2O_2 solution, the Cu cap catalyzes the H_2O_2 degradation on one side of the particle and therefore creates an unbalanced distribution of product ions, which leads to a fluid flow propelling the particle towards the copper cap direction (Figure 2 B). Based on the excellent agreement that we found between the behaviour of these particles in external flows and simulations using a self-electrophoretic

mechanism in our previous work, we assume different catalytic activities between the equator and the pole of the copper cap that cause an electric field similar to[22] and build a finite numerical simulation model by COMSOL (Figure 2 D).

In the previously described microfluidic setup, two reservoirs containing water and a solution of 2.5 % hydrogen peroxide were pressurized using an Elveflow pressure controller. The suspension of active particles was then injected with a syringe into the water streamline prior to the microfluidic chip. The two streams were then injected into the microfluidic chip at a constant flow rate of 80 μL/min until a stable gradient of H_2O_2 was established in the chamber. The flow was then stopped and videos were recorded in the field of view around the middle of the chamber, where the gradient was formed (Figure 2 A). A control experiment was done by replacing the medium of the microswimmers (i.e. water) with hydrogen peroxide to remove any gradient but still keep the activity. Particles' trajectories were extracted from the recorded videos using a homemade tracking software in Matlab.

A number of selected particle trajectories are illustrated on Figure 3. The Cu cap of the Janus sphere is easily identified with brightfield microscopy and this allowed to recover the particles orientation. When plotting the cap orientation angle of at least 200 particles in the presence and absence of H_2O_2 gradient, a clear difference is noticeable. In the control experiment, the orientation of motion is isotropic, there is no preferred direction (Figure 3 A.iii). On the other hand, in the presence of a gradient, a significant anisotropy is visible along the gradient (Figure 3 B.iii). Indeed, the microswimmers are swimming strongly upward the gradient, towards the more concentrated area. There is
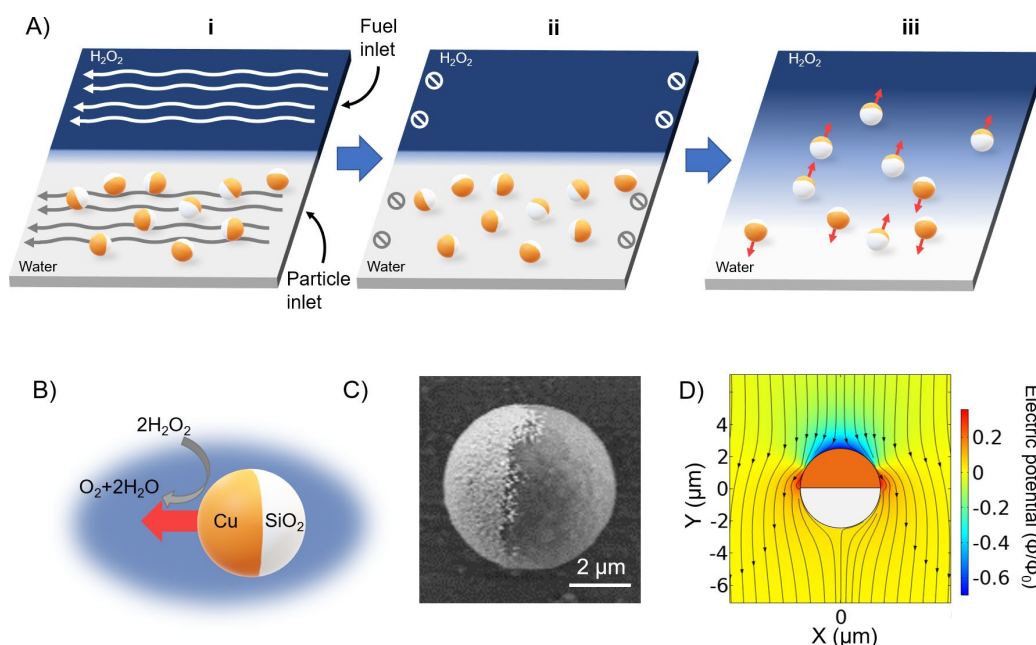

Figure 2. Intrinsic propulsion and chemotaxis of Cu@SiO$_2$ micromotors. A) Operating principles of the positive and negative chemotaxis of Cu@SiO$_2$ micromotors. B) Schematic diagram of the intrinsic propulsion of Cu@SiO$_2$ micromotors in H_2O_2. C) Scanning electrical micrograph of a Cu@SiO$_2$ microsphere. D) Electric potential (color coded) and flow field lines (black arrows) around a Cu@SiO$_2$ Janus micromotors.
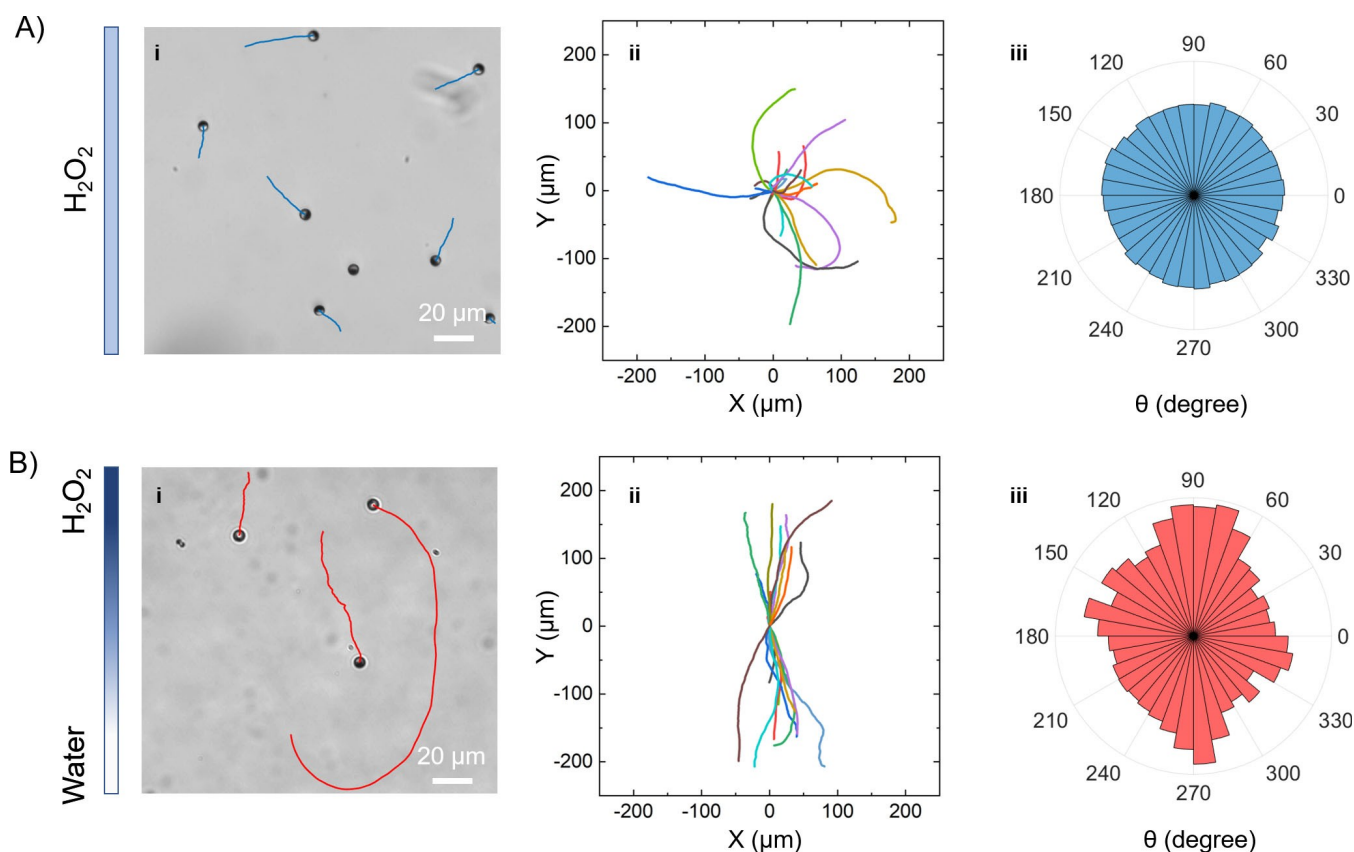
Figure 3. Statistical comparisons between chemotaxis and non-chemotaxis behaviors of Cu@SiO$_2$ micromotors. (i) Optical micrographs, (ii) trajectories and (iii) distribution of the directionality of Cu@SiO$_2$ micromotors moving in 2.5% H$_2$O$_2$ without gradient (A) and with the gradient (B).

also a clear, although slightly weaker, trend downward the gradient. To confirm this phenomenon, we investigated the chemotaxis behaviors at different concentrations of H$_2$O$_2$ (Figure S3). With the concentrations decreasing from 2.5% to 0.1%, the significant trends of upward and downward motion however still emerge at 0.5%, but then become indistinctive at 0.1%. The average speeds of particles in Figure S3 are also calculated and found to scale with the increasing H$_2$O$_2$ concentrations (Figure S4).

Discussion

The upward motion of active Janus particles towards the region of more concentrated fuel, also called positive chemotaxis, was first described by Baraban et al.[13] Using a flowing gradient, this study was not considering the (then unknown) potential cross-stream migration effect.[23] Using a pressure driven setup and a feedback loop, we managed to decouple both effects and clearly observed the chemotactic response of these particles. As expected, we found a symmetry in the behavior with both positive and negative chemotaxis being present in the same set of experiments. To help understand our findings, numerical simulations with COMSOL were made to model the flow field around the microswimmers in different configurations (Figure 4). De-

pending on their original orientation in the vicinity of the fuel gradient, the particles will experience forces and torques that will influence a change in their orientation. If the particles are initially oriented perpendicular to the flow, the cap facing the region more concentrated in peroxide, the chemical conversion is equal and symmetric on both sides of the cap; thus leading to a symmetric flow field around the particles and no forces changing their orientation apart from rotational diffusion. The same principles apply when the particles are oriented downward the gradient, the drag force exerted on them is uniform and does not induce any directional change thus explaining the great proportion of microswimmers swimming in this direction. The case at lower fuel concentrations could also be attributed to the corresponding weaker drag force, which can barely overcome the rotational diffusion of particles and reorient them along the gradient, hence leading to a more random moving direction and weaker propulsion speeds of particles.

However, this theory is insufficient to explain the results obtained and the clear asymmetry and higher proportion of particles oriented towards the 90 degree angle compared to the 270 degree angle. All particles in the gradient area that are not aligned parallel to the gradient will experience uneven drag forces. These forces will induce a torque that will reorient the particles' cap towards the 90 degree angle. The propulsion force being proportional to the amount of
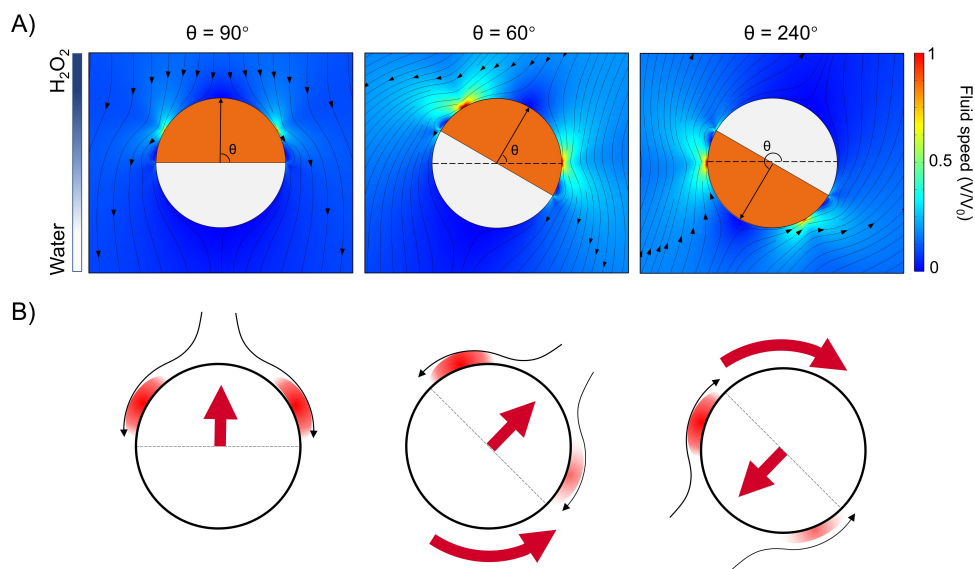
Figure 4. Finite element simulation of Cu@SiO$_2$ micromotors in a chemical gradient with different orientation configurations. A) Fluid speed magnitude (color coded) and flow field lines (black arrows) around a Cu@SiO$_2$ micromotor when the orientation of the particle aligns with the gradient ($\theta = 90°$) or deviate from it ($\theta = 60°$ and $\theta = 240°$). B) Schematic of the flow induced torque exerted on the particle forcing it to modify its orientation and align with the gradient direction.

product ions created during the chemical decomposition of H$_2$O$_2$, a higher concentration of fuel leads to a higher propulsion force and consequently, a higher drag force.

To verify this theory more explicitly, we analyze the moving direction changes during the chemotaxis behavior of particles (see Figure 5). By comparing the orientation of the Janus particles with the direction of motion, we confirm that both are correlated and that a change in orientation will induce a change in the velocity vector. Furthermore, we confirmed the underlying hypothesis that a change in orientation is immediately followed by a change in the velocity vector. Recent work have reported similar chemotaxis behavior by orientation rectification of ZnO micromotors.[24]

Popescu et al. published a report on chemotaxis, stating that a determining set of parameters for such behaviour is the contrast of surface mobilities.[25] Therein, they affirm a broadly supported[26] claim that since the active propulsion of swimmers depends on the fuel concentration, active particles should also be able to orient with respect to a fuel source. Popescu et al. differentiate into positive and negative chemotaxis, depending whether the particles orient towards or away from higher concentrations. While similar processes in biology are typically ascribed to a complex interplay of sensing and signal translation, Popescu et al. predict a rotation respective the gradient as response to a varying phoretic mobility across the particle surface. Because of different concentrations of certain solute molecules along
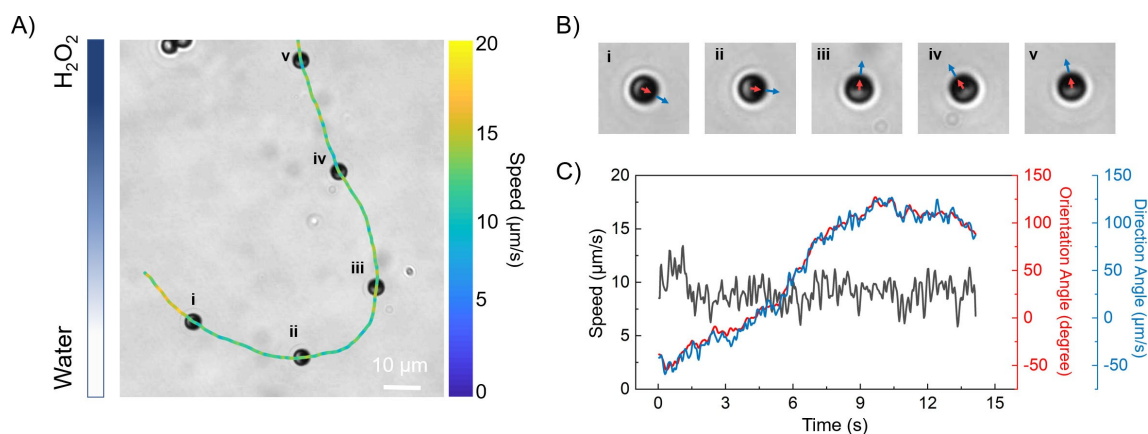

Figure 5. Orientation changes lead to apparent chemotaxis. (A) Representative trajectory of a Cu@SiO$_2$ micromotor changing its swimming direction to align with the gradient. (B) Direction (blue arrow) and orientation (red arrow) of the Cu@SiO$_2$ micromotor in (A) at different time intervals. (C) Instantaneous speeds, direction angles and orientation angles of the the Cu@SiO$_2$ micromotor in (A).

the particle surface, a flow is induced in the vicinity of the particles which is termed phoretic slip. The magnitude and direction of the flow depend on the material properties and the interactions with the solutes, which are summarized in the so called phoretic mobility. Popescu et al. predict, that depending on the contrast of surface mobilities, each Janus particle is characterized by a tendency to rotate either towards, or away from a chemical gradient.[25] Initially, our results seem to contradict this predictions, because approximately the same number of particles turn towards and away from the gradient. However, since it is very difficult to *a priori* predict the ratio of surface mobilities, there is no prediction whether Cu@SiO$_2$ particles belong to one group ('quadrant') that should orient to swim gradient up or the other. A detailed study of different Janus particles[27–29] or particles in different fuels[30] is beyond the scope of this manuscript but is required to broaden our understanding before making such conjectures.

Conclusion

Using pressure pumps to precisely control flow rates in a microfluidic gradient generation system, we successfully performed a fast stop-and-go flow experiment to study apparent chemotaxis of Janus microswimmers. We observed and studied the physical mechanisms behind the swimming pattern of copper coated silica microparticles in a gradient of hydrogen peroxide. By analyzing the orientation angle of the particles, a clear trend indicates both positive and negative chemotaxis. Studying the flow field surrounding the microswimmers using COMSOL simulations, we were able to describe the forces and torques applied on the particles when placed in a gradient as fuel, leading to a change in their orientation. Three main cases were identified: if the particles have their cap oriented towards the more concentrated region, no change in orientation is due to the gradient; if the cap is askew in the gradient, the particles will reorient its trajectory towards the high concentration; and finally, a particle oriented downward the gradient will not be affected by any torque and will keep its initial orientation. Further studies applying this technology to other types of microswimmers and fuels will be necessary to generalize the physical concepts.

Supporting Information

Supporting Information containing the experimental section, information on the numerical simulation, information on the supporting videos and additional information on established gradients and resulting angles, is available from the Wiley Online Library or from the author.

Acknowledgements

Conflicts of Interest

Two authors A.N. and B.G., at the time of this work, were employees of Elvesys SAS, a for profit company that sells Elveflow equipment, which was used for flow control and measurements in this work.

Data Availability Statement

The data that support the findings of this study are available from the corresponding author upon reasonable request.

Keywords:

[1] B. Chance, *Rev. Sci. Instrum.* **1951**, *22*, 619–627.
[2] C. R. Bagshaw in *Stopped-Flow Techniques* (Ed.: G. C. K. Roberts), Springer Berlin Heidelberg, Berlin, Heidelberg, **2013**, pp. 2460–2466.
[3] D. Dendukuri, S. S. Gu, D. C. Pregibon, T. A. Hatton, P. S. Doyle, *Lab Chip* **2007**, *7*, 818–828.
[4] G. M. Whitesides, *Nature* **2006**, *442*, 368–373.
[5] P. Sharan, A. Nsamela, S. C. Lesher-Pérez, J. Simmchen, *Small* **2021**, *17*, 2007403.
[6] V. Sourjik, N. S. Wingreen, *Curr. Opin. Cell Biol.* **2012**, *24*, 262–268.
[7] L. Stephens, L. Milne, P. Hawkins, *Curr. Biol.* **2008**, *18*, R485–R494.
[8] Y. Ji, X. Lin, Z. Wu, Y. Wu, W. Gao, Q. He, *Angew. Chem.* **2019**, *131*, 12328–12333; *Angew. Chem. Int. Ed.* **2019**, *58*, 12200–12205.
[9] K. K. Dey, X. Zhao, B. M. Tansi, W. J. Méndez-Ortiz, U. M. Córdova-Figueroa, R. Golestanian, A. Sen, *Nano Lett.* **2015**, *15*, 8311–8315.
[10] C. Lozano, C. Bechinger, *Nat. Commun.* **2019**, *10*, 2495.
[11] C. Lozano, B. Ten Hagen, H. Löwen, C. Bechinger, *Nat. Commun.* **2016**, *7*, 12828.
[12] L. Niese, L. Wang, S. Das, J. Simmchen, *Soft Matter* **2020**, *16*, 10585–10590.
[13] L. Baraban, S. M. Harazim, S. Sanchez, O. G. Schmidt, *Angew. Chem. Int. Ed.* **2013**, *52*, 5552–5556; *Angew. Chem.* **2013**, *125*, 5662–5666.
[14] K. K. Dey, S. Bhandari, D. Bandyopadhyay, S. Basu, A. Chattopadhyay, *Small* **2013**, *9*, 1916–1920.
[15] A. Somasundar, S. Ghosh, F. Mohajerani, L. N. Massenburg, T. Yang, P. S. Cremer, D. Velegol, A. Sen, *Nat. Nanotechnol.* **2019**, *14*, 1129–1134.
[16] S. Yu, Y. Cai, Z. Wu, Q. He, *View* **2021**, 20200113.
[17] J. Katuri, K. Seo, D. Kim, S. Sanchez, *Lab Chip* **2016**, *16*, 1101–1105.
[18] S. H. Lee, W. Kang, S. Chun, *Flow Meas. Instrum.* **2018**, *62*, 105–112.

[19] S. Saha, R. Golestanian, S. Ramaswamy, *Phys. Rev. E* **2014**, *89*, 062316.

[20] J. Agudo-Canalejo, P. Illien, R. Golestanian, *Nano Lett.* **2018**, *18*, 2711–2717.

[21] P. Sharan, Z. Xiao, V. Mancuso, W. E. Uspal, J. Simmchen, *Upstream rheotaxis of catalytic Janus spheres* **2021**, ChemRxiv preprint DOI: 10.26434/chemrxiv-2021-9s6wz.

[22] S. Ebbens, D. Gregory, G. Dunderdale, J. Howse, Y. Ibrahim, T. Liverpool, R. Golestanian, *EPL* **2014**, *106*, 58003.

[23] J. Katuri, W. E. Uspal, J. Simmchen, A. Miguel-López, S. Sánchez, *Sci. Adv.* **2018**, *4*, eaao1755.

[24] F. Mou, Q. Xie, J. Liu, S. Che, L. Bahmane, M. You, J. Guan, *Natl. Sci. Rev.* **2021**, *8*, nwab066.

[25] M. N. Popescu, W. E. Uspal, C. Bechinger, P. Fischer, *Nano Lett.* **2018**, *18*, 5345–5349.

[26] S. Saha, R. Golestanian, S. Ramaswamy, *Phys. Rev. E* **2014**, *89*, 062316.

[27] D. P. Singh, W. E. Uspal, M. N. Popescu, L. G. Wilson, P. Fischer, *Adv. Funct. Mater.* **2018**, *28*, 1706660.

[28] J. Simmchen, J. Katuri, W. E. Uspal, M. N. Popescu, M. Tasinkevych, S. Sánchez, *Nat. Commun.* **2016**, *7*, 10598.

[29] A. T. Brown, I. D. Vladescu, A. Dawson, T. Vissers, J. Schwarz-Linek, J. S. Lintuvuori, W. C. Poon, *Soft Matter* **2016**, *12*, 131–140.

[30] L. Feuerstein, C. G. Biermann, Z. Xiao, C. Holm, J. Simmchen, *J. Am. Chem. Soc.* **2021**, *143*, 17015–17022.